HIGH - TEMPERATURE CREEP BEHAVIOUR OF CAST COBALT-BASE SUPERALLOYS

Jiri DVORAK [1,2], Petr KRAL [1,2], Marie KVAPILOVA [1,2], Karel HRBACEK [1], Václav SKLENICKA [1,2]

[1]*Institute of Physics of Materials, Academy of Sciences of the Czech Republic, Brno, Czech Republic, EU*
dvorak@ipm.cz

[2]*CEITEC-IPM, Institute of Physics of Materials, Brno,Czech Republic, EU*
dvorak@ipm.cz

Abstract

Two cast and heat-treated NbC and TaC - strengthened cobalt superalloys have been developed for an investment casting of spinner discs for glass wool industry. In this work constant load creep tests in tension were carried out in argon atmosphere at three testing temperature 900, 950 and 1000 °C and at the initial applied stresses ranging from 40 to 200 MPa. All the tests were continued until the final fracture. The results of creep testing were combined with microstructural and fractographic examinations by means of light and scanning electron microscopy. A mutual comparison of creep characteristics of the investigated superalloys under comparable creep loading conditions showed that NbC-strengthened superalloy exhibited longer creep life than TaC-strengthened one. Further, it was found that carbide precipitation is the primary strengthening mechanism in both cobalt-base superalloys under investigation and the amount, morphology and type of carbides have the decisive effect on the creep properties including creep damage and fracture processes. By contrast, CoNb superalloy exhibited a more brittle character of creep fracture mode than CoTa superalloy due to a premature fracture. This study was initiated to investigate in more details operating creep deformation processes and the effect of the creep microstructure and damage evolution on both investigated superalloys. The different behaviour and properties of studied superalloys were explained based on the received results of this study.

Keywords: Co-base superalloys, creep tests, microstructure evolution, carbide precipitation, damage process

1. INTRODUCTION

Ni-base superalloys are highly valued for fabrication of high temperature components. These superalloys are mostly hardened by γ´ precipitates that are distributed uniformly in the γ matrix. This unique γ/ γ´ two-phase structure enables Ni-base superalloys to have excellent mechanical properties which include high-temperature strength and resistance to creep and fatigue [1-3]. Generally, Ni-base superalloys attain their outstanding properties from combination of solid solution, precipitation and grain boundary strengthening. In the course of our previous works a nickel-base superalloy of Ni-Cr-W-C system was developed, referred to as alloy 141I [4]. This alloy has very good mechanical properties and its service life exceeded worldwide commonly used alloys for cast of defibering heads. At present, however, chemical industry has required a new high-temperature materials working at operating temperatures exceeding the possibilities of Ni alloys. These requirements led us to the development of new type of superalloys. Cobalt exhibits a higher melting temperature than Ni and may be used as a principal element in new high temperature structural alloys and enables the possibility for Co superalloys to successfully compete with Ni-base alloy in terms of high temperature strength and creep resistance. Recently, two cast and heat-treated NbC and TaC - strengthened Co - base superalloys have been produced in company PBS Velka Bites a.s., Czech Republic, for an investment casting of spinner discs for glass wool industry. Solid solution strengthening of the matrix and carbide precipitation are the primary strengthening mechanisms in these cobalt-base superalloys and the amount, morphology and type of carbides

have the decisive effect on the mechanical properties. These high refractory complex carbides precipitate in the interdendritic regions of the matrix [5,6]. Previous studies suggested that the use of appropriate heat treatment can significantly influenced the mechanical properties of cobalt-base superalloys [3,7,8]. It is well known that primary carbides are unstable and tend to degenerate during high temperature heating [9]. Also, heating on creep temperature and creep exposure can lead to improvement or deterioration of mechanical properties due to dissolution of coarse primary carbides, precipitation of fine secondary carbides or carbide transformation. Different evolution of microstructure can lead to different development of creep damage and fracture. Therefore, it is essential to understand microstructural changes of the alloys during service at high temperature. The objective of present research is to compare creep properties of two cobalt-base superalloys. Simultaneously, investigations of the effect of the creep damage evolution and creep fracture mechanisms and modes in these alloys were performed.

2. EXPERIMENTAL MATERIALS

Cast Co-base superalloys resistant to high-temperature oxidation were processed in a foundry company PBS Velka Bites a.s., Czech Republic, using conical ingots with minimum diameter of 13 mm, maximum diameter of 18 mm and length of 90 mm. The chemical composition of the Co superalloys used in this work is given in **Table 1**. These alloys differ significantly in the presence of carbide-forming elements, the first contain Ta and the other Nb, so for further description we will mark them as CoTa alloy and CoNb one. Both Co-based superalloys were received in the state after casting with following solution annealing at 1150 °C / 90 min. Standard uniaxial tensile creep tests were carried out using cylindrical creep specimens with the gauge diameter of 3.5 mm and the gauge length of 50 mm. The creep tests were performed at applied stresses ranging from 40 to 200 MPa and at three testing temperature 900, 950 and 1000 °C. The creep elongations were continuously measured using a linear variable differential transducer, recorded digitally and computer processed. All creep specimens were run up to the final fracture. Following creep testing the microstructure and fracture features of ruptured creep specimens of Co alloys were examined using scanning electron microscopy.

Table 1 The chemical composition of studied superalloys (in wt. %)

	Composition [wt. %]									
	Co	**Ni**	**C**	**W**	**Cr**	**Fe**	**Ta**	**Nb**	**Si**	**Mn**
CoTa	Bal	23	0.6	7	29.3	4.9	2.3	x	1.0	0.22
CoNb	Bal	10.8	0.65	8	30.5	0.28	x	2.48	0.39	0.23

3. EXPERIMENTAL RESULTS AND DISCUSSION

3.1. Creep testing

Figures 1a displays the standard creep curves of Co superalloys for the tests conducted under constant tensile loads at temperatures of 900°C and 100 MPa. The results show, that at the same value of applied stress, the CoNb alloy exhibits better creep resistance than the CoTa alloy. Further, fracture elongation was dramatically increased for CoTa alloy and the value of minimum creep rate is over one order of magnitude higher than that of the CoNb alloy. It should be stressed that the standard creep curves do not often clearly indicate the individual stages of creep. However, these standard ε vs. t creep curves can be easily replotted in the form of the creep rate $\dot{\varepsilon}$ vs. time t (**Figure 1b**) or creep rate $\dot{\varepsilon}$ vs. strain ε (**Figure 1c**). It can be seen that shapes of the creep curves of particular alloys exhibit differences as well. The curve of the CoNb alloy exhibits a long

hardening in the primary part of creep curve followed by nearly stable strain rates over a long creep duration (**Figure 1b**). The accelerating tertiary part occurs at the very end of the creep test, leading to final fracture. CoTa alloy exhibits short primary stage which practically immediately pass into the tertiary one and this stage represents the dominant part of the creep exposure of this alloy. The creep elongation is characterized by an initial small instantaneous loading strain followed by a transient (primary) creep for both states as seen in **Figure 1c**. The gradual accumulation of creep strain in the following tertiary creep is observed at CoTa alloy, whereas rapid creep strain accumulation is observed in the tertiary creep of CoNb alloy just prior to final fracture. **Figure 2** shows the same creep characteristics for temperature of 1000 °C and stress of 60 MPa. Similarly, CoNb alloy exhibits better creep resistance and lower creep final elongation in comparison to CoTa one. Simultaneously, creep curves show, that the time of hardening in primary stage is larger compared with softening part in tertiary stage for both alloys. Since the microstructure evolution is very similar in both superalloys, the decreased creep strength of CoTa superalloy is mainly results of reduced effect of the solid solution strengthening due to lower Co content in the CoTa ally matrix (**Table 1**).

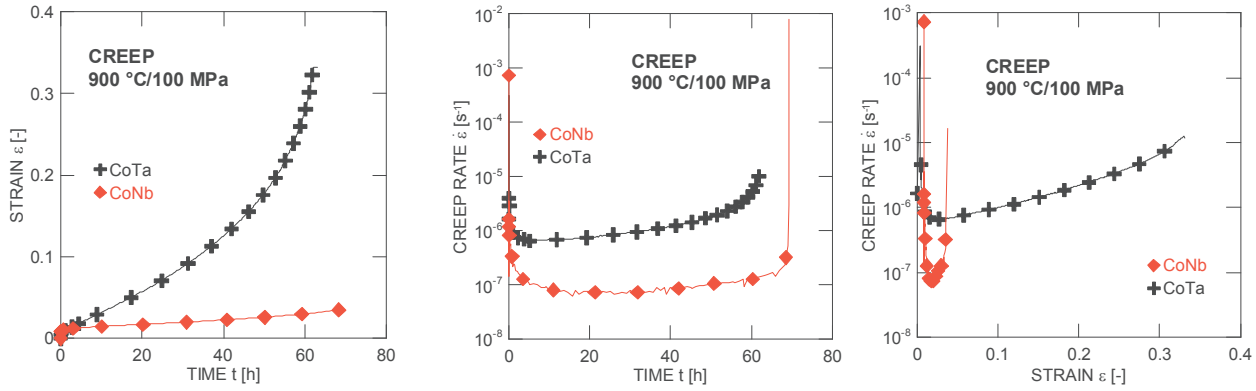

Figure 1 Creep curves for the cobalt superalloys at temperature 900 °C and 100 MPa: (a) standard creep curves ε vs. t, (b) creep rate $\dot{\varepsilon}$ vs. time t, and (c) creep strain ε vs. creep rate $\dot{\varepsilon}$

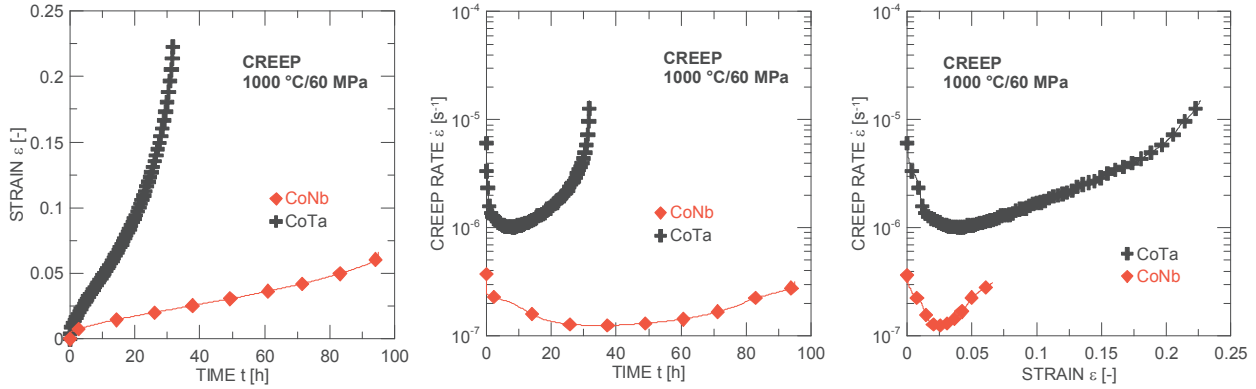

Figure 2 Creep curves for both Co-base superalloys at temperature 100 °C and 60 MPa: (a) standard creep curves ε vs. t, (b) creep rate $\dot{\varepsilon}$ vs. time t, and (c) creep strain ε vs. creep rate $\dot{\varepsilon}$

In the present work, the minimum creep rate and the time to fracture data are re-analysed to find out whether the time to fracture t_f is controlled by the same process(es) and/or mechanism(s) as creep deformation. The minimum creep rate $\dot{\varepsilon}_m$, is a function of temperature T, the applied stress σ and microstructure s, as

$$\dot{\varepsilon}_m = \dot{\varepsilon}_m (T,\sigma,s). \quad (1)$$

The dependence of the minimum creep rate on the applied stress can be characterized by the apparent stress exponent of the minimum creep rate to applied stress, n, which is defined as

$$n = [(\partial \ln \dot{\varepsilon}_m / \partial \ln \sigma)]_T \quad (2)$$

Similarly, the stress exponent of the time to fracture, m, can be written as

$$m = - [(\partial \ln t_f / \partial \ln \sigma)]_T. \quad (3)$$

In **Figure 3**, the minimum creep rates $\dot{\varepsilon}_m$ are plotted against the applied stress σ on a bilogarithmic scale for various testing temperatures ranging from 900 to 1000 °C, Inspection of **Figure 3** leads to an observation that the stress dependences of the minimum creep rates for both alloys at various stresses show a similar trend. The slopes and, therefore, the apparent stress exponents of the minimum creep rate was evaluated as n=8. Simultaneously, the stress exponent of the time to fracture illustrated by **Figure 4** was obtained as m=7 for both alloys and temperatures. Similarity of these values indicates, that both the creep deformation and fracture are controlled by the same mechanism(s) which is(are) probably dislocation (power-law) creep in particle strengthened alloys, where the main rate controlling creep deformation mechanism should be dislocation glide; that is, the creep behaviour is dominated by the interaction between dislocations and obstacles such as precipitates.

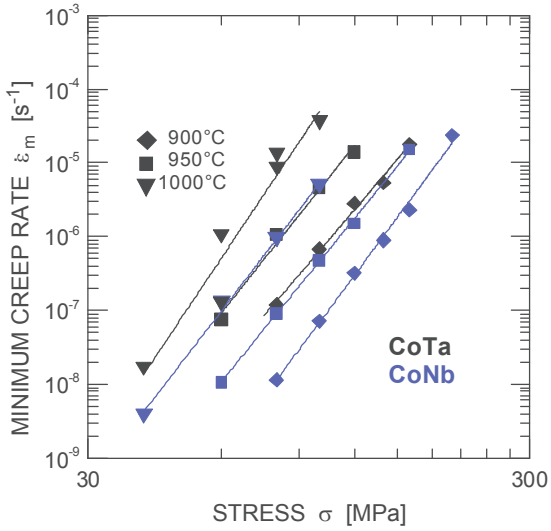

Figure 3 Stress dependences of the minimum creep rate for different temperatures

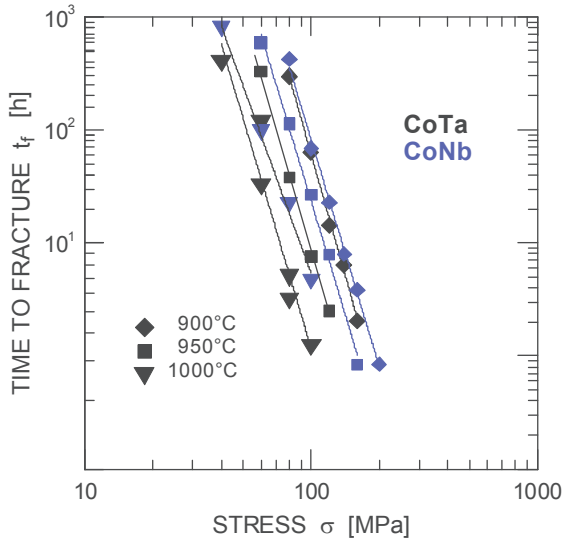

Figure 4 Stress dependences of the time to fracture for different temperatures

3.2. Microstructure of Co-base superalloys

3.2.1. Microstructure of as-received state

Microstructure in as-received condition (after casting and solution annealing) for both alloys are given in **Figure 5**. For identification of particular phases, energy dispersion X-ray (EDX) analysis were carried out. The microstructure contains a Co-Ni-Cr-W matrix formed by solid solution and two types of primary complex carbides and/or eutectics, (W, Cr)-rich $M_{23}C_6$ and Chinese script MC with presence of Ta or Nb. Both $M_{23}C_6$ and MC carbides are situated at grain boundaries and in interdendritic regions, forming a continuous network around the columnar grained matrix. It can be assumed that primary carbides generally dissolved in the matrix during solution annealing. But in our case, it cannot be excluded that not all carbides were fully dissolved due to short time of annealing (**Figure 5b**). Besides these $M_{23}C_6$ precipitates, secondary fine phase was detected, which preferentially precipitated in the closed proximity of primary $M_{23}C_6$. Further, EDX analysis revealed tungsten-rich M_6C carbides (illustrated by bright white colour.)

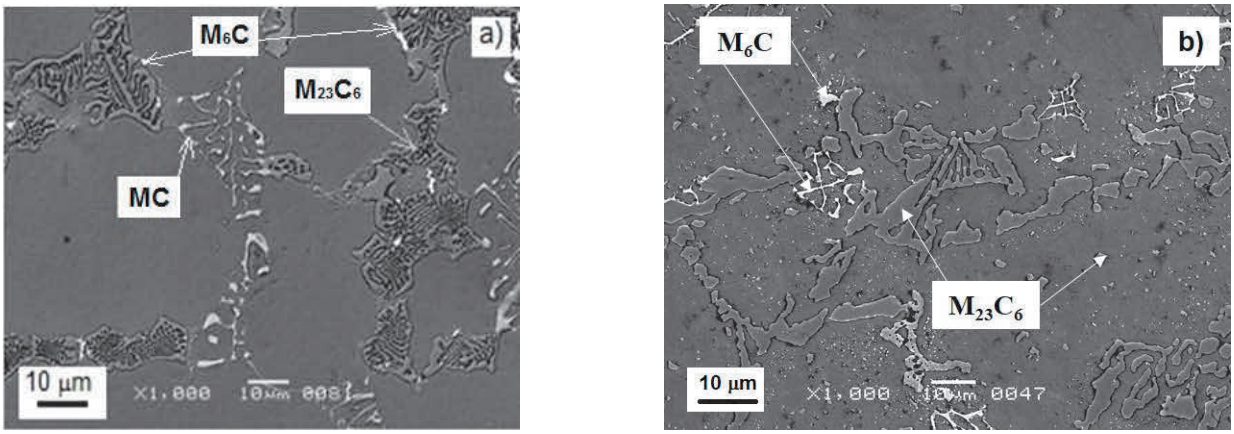

Figure 5 SEM microstructure of a) CoNb and b) CoTa superalloys

3.2.2. Microstructure after creep exposures

Our creep testing at lower temperature (up to 1000 °C) do not lead to complete dissolution of primary carbides but the precipitation of fine secondary carbide $M_{23}C_6$ can happened**.** The secondary $M_{23}C_6$ precipitation is closely related to the decomposition from the matrix during creep exposition. **Figure 6** shows the microstructure of both alloys after creep exposition at 1000 °C. During creep exposure, the fine carbide can be observed in **Figure 6a**. These precipitates are unevenly distributed. There is a dense distribution around the primary lamellar carbides and a rare distribution in the center of grains. However, it can be assumed that such (high) temperatures do not allow the precipitation of the secondary phase. In last, structural stability of CoNb alloy was examined by isothermal stress-free annealing at temperatures 900 -1100 °C for 100h [10]. It has been reported, that since to beginning of annealing, the precipitation of fine secondary $M_{23}C_6$ carbides close to eutectic carbide skeleton occurred. With continuing annealing time, the amount of secondary carbides increases followed with coarsening. However, temperature above 1000 °C led to finer carbide dissolution. Simultaneously, the volume fraction of primary carbides does not change dramatically compared with the as-cast state at temperature up to 1100 °C.

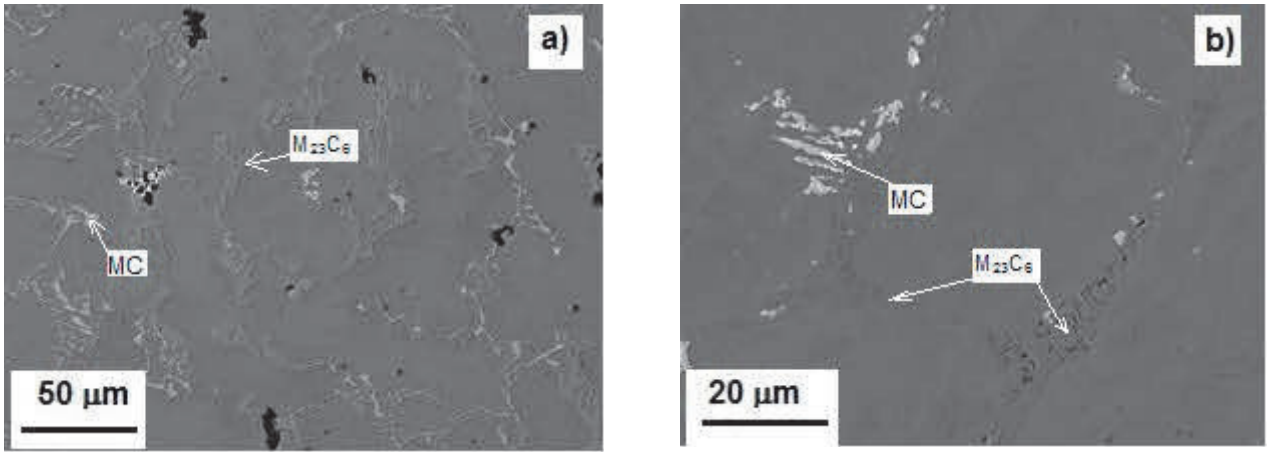

Figure 6 SEM microstructure of a) CoNb, and b) CoTa superalloy after creep at 1000 °C and 40MPa

It is obvious, that different creep fracture ductility of both superalloys could be explained by different way of the formation and development of creep damage and fracture. The change in fracture mode is associated with a change in damage initiation mechanisms. The damage development closely connected with an interaction between matrix and primary carbides are mostly the main sites for the main crack propagation. In CoNb superalloy, the brittle fracture was caused by creep cavitation, decohesion at particle/matrix and cracking of

primary carbides and eutectics creating fracture path, while the ductile fracture in CoTa superalloy is relevant to damage by local loss of internal section of the specimen (necking) due to instability of plastic deformation.

4. CONCLUSIONS

Creep results showed that under the same test conditions CoNb superalloy exhibited lower minimum creep rate value, longer creep life but lower elongation than CoTa superalloy. The very similar values of the exponents n and m indicate that the creep deformation and fracture are controlled by the same mechanism. Together with solid solution strengthening of the matrix very important mechanism is precipitation strengthening by complex carbides. It was observed, that whereas in CoNb superalloy is the final brittle fracture caused by cavitation damage coalescence and creep crack growth, in the case of CoTa superalloy ductile creep fracture caused by loss of stability plastic deformation of matrix occurred.

ACKNOWLEDGEMENTS

This work was financially supported by Ministry of Industry and Trade of the Czech Republic within the framework programme MPO Trio under the project No. FV10699. The experimental facilities of IPMinfra supported through project No. LM2015069 of MEYS and CEITEC - Central European Institute of Technology supported by the project CZ.1.05/1.1.00/02.0068 financed from European Regional Development Fund were used. We are grateful to Dr. Jiří Zýka of UJP PRAHA a.s., Czech Republic, EU, for stimulating discussion.

REFERENCES

[1] GU, Y., HARADA, H., CUI, Ch., PING, D., SATO, A.., FUJIOKA, J. New Ni-Co-base disc superalloys with higher strength and creep resistance. *Scripta Mater.,* 2006, Vol 55, pp 815-818.

[2] ZHANG, J., MURAKURO, T., KOIZUMI, Y., KOBAYASHI, T., HARADA, H., MASAKI, S. Interfacial Dislocation Networks Strengthening a Fourth-Generation Single-Crystal TMS-138 Superalloy. *Metall. and Mater. Trans. A,* 2002. vol. 33A, no 12, pp 3741-3746.

[3] KOBLE M., NEUKING K., EGGELER G. Dislocation reactions and microstructural instability during 1025 °C shear creep testing of superalloy single crystals. *Mater.Sci.Eng.*, 1997. Vol. A234-236, pp. 877-879.

[4] KVAPILOVA, M., KUCHAROVA, K., SKLENICKA, V., SVOBODA, M., HRBACEK, K., Creep behaviour and microstructural changes of model cast Ni-Cr-W-C alloys. *Procedia Engineering,* 2011. vol. 10, pp. 839-844.

[5] SIMS, T. C., HAGEL, W. C. *The superalloys: Cobalt-base Alloys*. New York: John Wiley & Sons, NY, 1972. 614 p.

[6] POLLOCK, T., TIN, S. Nickel-based superalloys for advanced turbine engines: chemistry, microstructure and properties. *J. Propul. Power,* 2006. vol. 22, pp. 361-374.

[7] JIANG, W., GUAN, H., HU, Z. Development of a heat treatment for a directionally solidified cobalt-base superalloy. *Metall. Mater. Trans*. A, 1999, vol. 30, pp. 2251-2254.

[8] GUI, W., ZHANG, H., YANG, M., JIN, T., SUN, X., ZHENG, Q. Influence of type and morphology of carbides on stress-rupture behaviour of a cast cobalt-base superalloy. *Journal of Alloys and Compounds,* 2017. vol. 728, pp. 145-151.

[9] GUI, W., ZHANG, H., YANG, M. The investigation of carbides evolution in a cobalt-base superalloy at elevated temperature. *J. Alloys. Compd.,* 2017. vol. 695, pp.1271-1278.

[10] PODHORNA, B., ANDRSOVA, I., DOBROVA, J., VODAREK, V., HRBACEK, K., Structure stability of Ni-base and Co-base alloys. *Mat. Sci. For.,* 2014. vol. 782, pp. 431-436.